Nanostructures

Deutsche Ausgabe: DOI: 10.1002/ange.201601947
Internationale Ausgabe: DOI: 10.1002/anie.201601947

Controlling the Atomic Structure of Au_{30} Nanoclusters by a Ligand-Based Strategy

*Tatsuya Higaki, Chong Liu, Chenjie Zeng, Renxi Jin, Yuxiang Chen, Nathaniel L. Rosi, and Rongchao Jin**

Abstract: *We report the X-ray structure of a gold nanocluster with 30 gold atoms protected by 18 1-adamantanethiolate ligands (formulated as $Au_{30}(S\text{-}Adm)_{18}$). This nanocluster exhibits a threefold rotationally symmetrical, hexagonal-close-packed (HCP) Au_{18} kernel protected by six dimeric $Au_2(SR)_3$ staple motifs. This new structure is distinctly different from the previously reported $Au_{30}S(S\text{-}^tBu)_{18}$ nanocluster protected by 18 tert-butylthiolate ligands and one sulfido ligand with a face-centered cubic (FCC) Au_{22} kernel. The $Au_{30}(S\text{-}Adm)_{18}$ nanocluster has an anomalous solubility (it is only soluble in benzene but not in other common solvents). This work demonstrates a ligand-based strategy for controlling nanocluster structure and also provides a method for the discovery of possibly overlooked clusters because of their anomalous solubility.*

Atomically precise gold nanoclusters have received wide attention owing to the importance of understanding the transitions in properties from small molecules to plasmonic nanoparticles.[1–9] The potential of metal nanoclusters in applications such as catalysis[10–12] is also a major driving force for the creation of nanoclusters with controlled structures. With respect to thiolate-protected gold nanoclusters, major advances have been achieved recently in the identification of aesthetic structural patterns.[13–15] However, the relationship between the structure of nanoclusters and the protecting ligand still remains elusive. Among the ligand effects, ligand bulkiness has been well recognized to be quite influential on the structure and size of nanoclusters,[16–18] whereas the aromaticity seems less critical, at least in the demonstrated case of $Au_{36}(SR)_{24}$ with different –R groups.[19,20] It was also found that the substituted benzenethiolates provide an effective means for tailoring the size and structure of nanoclusters.[5a,13] Nevertheless, it remains necessary to further investigate how to control the nanocluster structure and gain insights into the major factors that dictate the atomic structure of nanoclusters.

Herein we report a strategy that uses bulky 1-adamantanethiol (HS-Adm) to control the structure of a 30-atom gold nanocluster formulated as $Au_{30}(S\text{-}Adm)_{18}$. It is worth noting that a relevant nanocluster, $Au_{30}S(S\text{-}^tBu)_{18}$ (where ^{t}Bu represents *tert*-butyl), which has an extra sulfido atom and also a different carbon tail of ligand, was previously reported.[21,22] Our present work demonstrates the importance of ligands in controlling the metal core structure.

The synthesis of $Au_{30}(S\text{-}Adm)_{18}$ was performed by using a facile one-phase spontaneous size-focusing method.[23,24] Details of the synthetic procedure are described in the Experimental Section. Briefly, $HAuCl_4{\cdot}3H_2O$ and $[(C_8H_{17})_4N]^+Br^-$ were first dissolved in methanol, and then Au^{III} was reduced to Au^I with HS-Adm, followed by further reduction with $NaBH_4$. The initially polydisperse $Au_n(SR)_m$ nanoclusters underwent spontaneous size-focusing when the solution was stirred over a period of one week, which eventually led to predominant $Au_{30}(S\text{-}Adm)_{18}$ nanoclusters. After washing the crude product with methanol and dichloromethane three times, respectively, pure $Au_{30}(S\text{-}Adm)_{18}$ nanoclusters were extracted with benzene. The synthetic yield was approximately 20% (based on Au atoms). Single-crystal growth of the Au_{30} nanoclusters was performed by vapor diffusion of cyclohexane into a benzene solution of the nanoclusters.

The structure of the clusters was solved by single-crystal X-ray crystallography. The crystal shows an interesting face-centered cubic (FCC) arrangement of Au_{30} nanoclusters (Figure 1A), with eight nanoclusters at the cubic corners and six on the face centers of the cubic unit cell. This is the first reported example of gold nanoclusters packed into an FCC superstructure, although conventional nanoparticles often pack into FCC superlattices.[25] The atomic structure of the individual $Au_{30}(S\text{-}Adm)_{18}$ nanocluster is shown in Figure 1B (top view) and Figure 1C (side view).

The $Au_{30}(S\text{-}Adm)_{18}$ nanocluster possesses an Au_{18} inner core (or kernel) protected by six dimeric $Au_2(SR)_3$ staples in C_3 symmetry (Figure 2). Out of the six dimeric staples, three connect the first and third layers of the kernel (Figure 2A for top view and Figure 2C for side view). The remaining three dimeric staples connect the second and fourth layers in a similar fashion (Figure 2B and 2D) but rotate along the C_3 axis by 60° with respect to the former three dimeric staples. The overall core and staple structure is achiral since it also has an inversion center *i* and belongs to the S_6 point group.

The Au_{18} kernel comprises four layers (i.e., Au_3-Au_6-Au_6-Au_3) in an *a-b-a-b* manner with a hexagonal-close-packed

[*] T. Higaki, C. Zeng, R. Jin, Y. Chen, Prof. R. Jin
Department of Chemistry, Carnegie Mellon University
Pittsburgh, PA 15213 (USA)
E-mail: rongchao@andrew.cmu.edu
C. Liu, Prof. N. L. Rosi
Department of Chemistry, University of Pittsburgh
Pittsburgh, PA 15213 (USA)
R. Jin
School of Chemistry, Northeast Normal University
Changchun, Jilin 130024 (China)

Supporting information for this article can be found under: http://dx.doi.org/10.1002/anie.201601947.

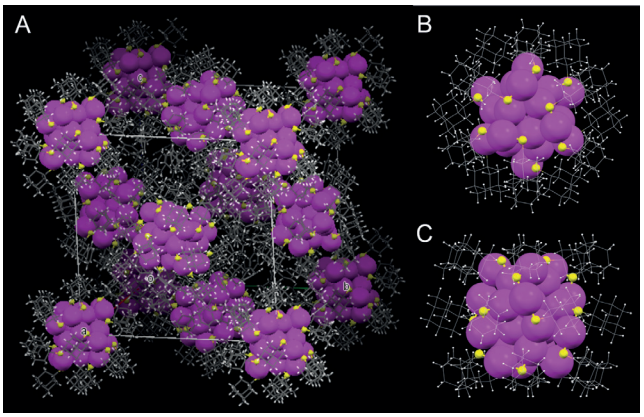

Figure 1. Overall structure of the $Au_{30}(S\text{-}Adm)_{18}$ nanocluster: A) Unit cell with a FCC superlattice arrangement; B) top view; C) side view. Labels: magenta = Au, yellow = S, gray = C, white = H. The carbon tails are in wireframe mode.

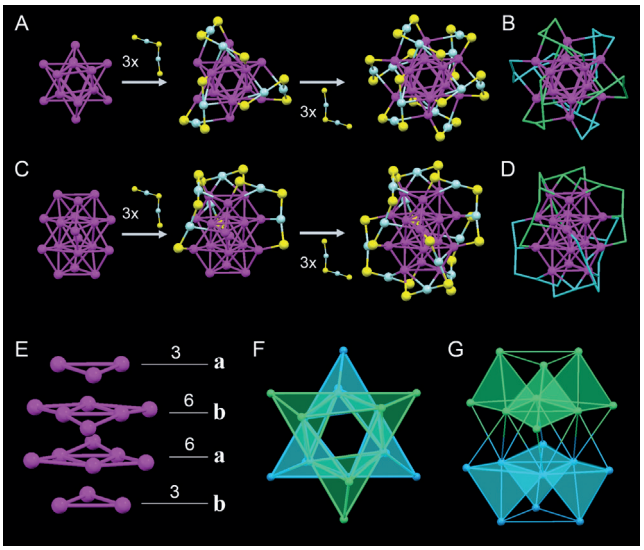

Figure 2. Anatomy of the structure of $Au_{30}(S\text{-}Adm)_{18}$ nanocluster: A, B) Top view of the Au_{18} kernel and the addition of six dimeric staple motifs in two steps (in blue and green, respectively); C, D) Side view of the kernel and addition of six staples; E) Four-layer structure of the Au_{18} kernel in a HCP manner; F, G) Six-Au_4 assembled pattern in top and side views. Color labels: magenta = Au in the kernel, light blue = Au in the staple, yellow = S.

(HCP) structure (Figure 2E) and has quasi-D_{3d} symmetry. From another perspective, the Au_{18} kernel can be viewed as an assembly of six tetrahedral Au_4 units (Figure 2F–G), evidenced by the distribution of Au–Au bond distances (Figure S1). Such an interpretation is based on the previous structural understanding of experimentally determined patterns of Au_4 tetrahedra[14b,26] and theoretically analyzed superatom network or complex models.[27,28] From this point of view, each Au_4 unit requires two valence electrons, and thus the total number of valence electrons in the nanocluster is $2e \times 6(\text{tetrahedra}) = 12e$, consistent with the value of 30(gold atoms)−18(ligands) = 12e. The 12e system has also been observed in the Au_{20} kernel of the $Au_{36}(SR)_{24}$ nanocluster[29] and the Au_{17} kernel of the $[Au_{23}(C{\equiv}C{-}Ph)_9(PPh_3)_6]^{2+}$ nanocluster[30] protected by mixed alkynyl and phosphine ligands. These nanoclusters also contain six tetrahedral Au_4 units in a different arrangement compared with the $Au_{30}(S\text{-}Adm)_{18}$ nanocluster in the current work, and such arrangements reflect how these isoelectronic 12e nanoclusters can be fabricated by arranging Au_4 units in different manners.

It is worth noting that theoretical works predicted $Au_{30}(S\text{-}^tBu)_{18}$[21] and $Au_{30}(SH)_{18}$[31] structures to comprise Au_{20} kernels of different configuration protected by different surface units. However, the observed structure in our current work of $Au_{30}(S\text{-}Adm)_{18}$ is completely different from those predicted structures. The observed $Au_{30}(S\text{-}Adm)_{18}$ structure also differs from the previously reported X-ray structure of $Au_{30}S(S\text{-}^tBu)_{18}$ (abbreviated as $Au_{30}S$ hereafter) despite the same numbers of gold atoms and thiolate ligands[21,22] (Figure 3).

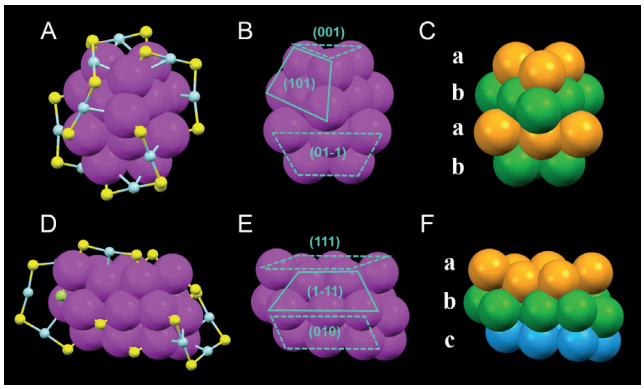

Figure 3. Comparison of the $Au_{30}(S\text{-}Adm)_{18}$ and $Au_{30}S(S\text{-}^tBu)_{18}$ structures (carbon tails omitted). A) Au_{18} kernel and staples; B) Au_{18} core only; C) Au_{18} core of HCP arrangement in $Au_{30}(S\text{-}Adm)_{18}$; and D) Au_{22} core and staples; E) Au_{22} core only; F) Au_{22} core of FCC arrangement in $Au_{30}S(S\text{-}^tBu)_{18}$.

The $Au_{30}S$ nanocluster comprises an Au_{22} kernel protected by six bridging thiolate, two monomeric staples, two trimeric staples, and one sulfido unit on the surface (Figure 3D). The Au_{22} kernel structure in the $Au_{30}S$ evolves from the FCC Au_{20} kernel in the $Au_{28}(SPh\text{-}^tBu)_{20}$ nanocluster[32] reported earlier. The structural difference in the Au_{30} core is quite intriguing in light of the structural similarity of 1-adamantanethiolate and *tert*-butyl thiolate, both ligands having similar S–C bond lengths (1.83 ± 0.01 Å vs. 1.838 ± 0.004 Å) and almost the same environment around the S atom bonded to gold.

The UV/Vis absorption spectrum of the $Au_{30}(S\text{-}Adm)_{18}$ nanoclusters shows distinct peaks at 368 and 550 nm (Figure 4). These spectral features can be distinguished from the single-peak (620 nm) profile of both the $Au_{30}S$ and $Au_{30}(S\text{-}^tBu)_{18}$ nanoclusters[17b,21] (Figure S2). The MALDI mass spectrum of the pure nanoclusters shows a single intact peak and no fragmentation was observed (Figure S6). In previous work[21] Crasto et al. speculated that $Au_{30}(S\text{-}^tBu)_{18}$ was converted to $Au_{30}S(S\text{-}^tBu)_{18}$ during the crystallization process but the sulfido source was unclear. We performed ligand exchange of the $Au_{30}(S\text{-}Adm)_{18}$ nanoclusters with *tert*-butyl thiol as well as treatment with Na_2S in attempts to

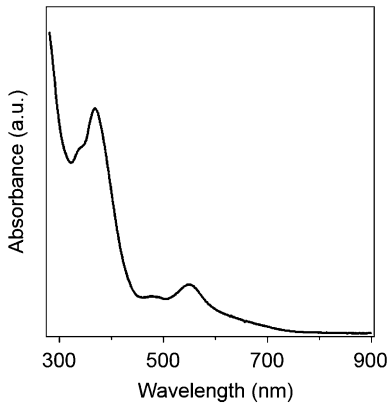

Figure 4. UV/Vis absorption spectrum of $Au_{30}(S\text{-}Adm)_{18}$ in benzene.

obtain $Au_{30}S(S\text{-}Adm)_{18}$, but the nanocluster was decomposed and both trials did not produce the expected nanocluster.

In recent work, the carbon tail structure of the thiolate ligand was considered to be the reason for structural transformation, rather than electronic conjugation between the benzene ring and the sulfur atom in the thiolate ligand.[5a,12] For example, a process of ligand-induced, thermally reversible isomerization was observed between two thiolate-protected 28-gold-atom nanoclusters, $Au_{28}(SC_6H_{11})_{20}$ and $Au_{28}(SPh\text{-}^tBu)_{20}$.[12] In the current work, 1-adamantanethiol is different from *tert*-butyl thiol in terms of the β-carbon environment and the β position also seems to play an important role in dictating the nanocluster structure, but further insights require theoretical analysis.[33] The structural difference between $Au_{30}(S\text{-}Adm)_{18}$ and $Au_{30}S$ might also be affected by the extra sulfido atom on the cluster surface, as in the case of body-centered cubic (BCC) $Au_{38}S_2(S\text{-}Adm)_{20}$ versus biicosahedral $Au_{38}(SCH_2CH_2Ph)_{24}$,[34] rather than the interaction of carbon tails in the ligand,[12] because sulfido directly connects to the kernel of the nanocluster and affects the stability of the electronic structure.[34]

In terms of thermal treatment, Au nanoclusters protected by tertiary thiolate, such as 1-adamantanethiolate and *tert*-butyl thiolate, can be classified into two groups: the nanoclusters with sulfido atoms such as $Au_{30}S(S\text{-}^tBu)_{18}$ and $Au_{38}S_2(S\text{-}Adm)_{20}$,[34] and the nanoclusters without sulfido atoms such as $Au_{24}(S\text{-}Adm)_{16}$[35] and $Au_{30}(S\text{-}Adm)_{18}$ from this work. Considering the available examples so far, the $Au_{30}(S\text{-}Adm)_{18}$ and $Au_{24}(S\text{-}Adm)_{16}$ do not have sulfido atoms, and both clusters are synthesized without any thermal treatment. On the other hand, the FCC $Au_{30}S(S\text{-}^tBu)_{18}$ and the BCC $Au_{38}S_2(S\text{-}Adm)_{20}$ possess sulfido atoms on the surfaces and both synthetic procedures involve thermal conditions. Without any sulfido source (e.g., Na_2S[22]), the sulfido atoms should come from the S–C bond cleavage of thiolate during the thermal process. The observation of this cleavage phenomenon in 1-adamantanethiolate and *tert*-butyl thiolate is reasonable considering the stability of tertiary carbocation. The absence of sulfido atoms in the $Au_{30}(S\text{-}Adm)_{18}$ synthesized at room temperature gave additional evidence for the formation mechanism of sulfido atoms at high temperatures.

With respect to the formation process of $Au_{30}(S\text{-}Adm)_{18}$, spontaneous size-focusing was observed, evidenced by the appearance of distinct absorption peaks in the UV/Vis spectra of the crude product over time and concurrent conversion of polydisperse $Au_n(SR)_m$ species to monodisperse $Au_{30}(S\text{-}Adm)_{18}$ in the mass spectra (Figures S3, S4). It is also worth mentioning that the $Au_{30}(S\text{-}Adm)_{18}$ nanocluster is insoluble in dichloromethane, evidenced by the absence of $Au_{30}(S\text{-}Adm)_{18}$ cluster signals in the mass spectrum of dichloromethane-extracted solute from the crude product (Figure S5), although dichloromethane is a widely used solvent for organic thiolate-protected Au nanoclusters as well as other clusters protected by 1-adamantanethiolate.[34] This peculiar solubility of $Au_{30}(S\text{-}Adm)_{18}$ is indeed important as it allows us to purify the nanocluster by removing by-products with dichloromethane, while in the final extraction with benzene, pure $Au_{30}(S\text{-}Adm)_{18}$ clusters can be selectively extracted from the product. For other common solvents, $Au_{30}(S\text{-}Adm)_{18}$ is slightly soluble in toluene and chloroform, but almost insoluble in tetrahydrofuran, acetone, acetonitrile, and dichloromethane. The successful synthesis of $Au_{30}(S\text{-}Adm)_{18}$ provides a clue for the discovery of new nanoclusters which may have been overlooked as insoluble residue with other impurities.

In conclusion, structural control of the Au_{30} nanocluster is realized by exploring the bulky adamantanethiol ligand. The new cluster is obtained in 20% yield (Au atom basis) via spontaneous size focusing under mild conditions that do not lead to any sulfido ligand as in the previously reported $Au_{30}S(S\text{-}^tBu)_{18}$ and $Au_{38}S_2(S\text{-}Adm)_{20}$. The newly obtained $Au_{30}(S\text{-}Adm)_{18}$ nanocluster shows distinct optical absorption features and peculiar solubility. The structure of $Au_{30}(S\text{-}Adm)_{18}$ is rather different from the previously reported $Au_{30}S(S\text{-}^tBu)_{18}$ cluster and also the theoretical structures of $Au_{30}(SH)_{18}$ and $Au_{30}(S\text{-}^tBu)_{18}$. The structural control of the Au_{30} nanocluster provides new insight into the intriguing relationships between the metal core and the protecting ligands of the nanoclusters.

Experimental Section

$[Au_{30}(S\text{-}Adm)_{18}]$: In a typical reaction, $HAuCl_4{\cdot}3H_2O$ (0.3 mmol, 118 mg) and tetraoctylammonium bromide (TOAB, 0.348 mmol, 190 mg) were dissolved in methanol (15 mL) in a 50 mL round-bottom flask. After vigorously stirring for 15 min, the color of the solution changed from yellow to reddish orange. Then, 1-adamantanethiol (1.6 mmol, 269 mg dissolved in 5 mL of methanol) was added dropwise to the mixture at room temperature. The reddish-orange solution gradually turned yellowish-white, indicating the conversion of Au^{III} to Au^{I} complexes. After approximately 15 min, $NaBH_4$ (3 mmol, 114 mg freshly dissolved in 6 mL of cold Nanopure water) was rapidly added to the solution under vigorous stirring. The solution turned black immediately, indicating formation of Au clusters, which then precipitated out of the methanol solution. After stirring for 1 week, the colorless supernatant was discarded and black sticky precipitate was collected. The precipitate was washed with methanol three times to remove excess thiol and then washed with dichloromethane. The nanoclusters were extracted from the residue with benzene. The yield was approximately 20% (based on Au atoms). Crystal growth was performed by vapor diffusion of cyclohexane into a benzene solution of clusters. Details of X-ray analysis are provided in the Supporting Information.

Acknowledgements

This work was financial supported by the AFOSR under AFOSR Award No. FA9550-15-1-9999 (FA9550-15-1-0154).

Keywords: gold · ligands · nanoclusters · nanostructures · thiols

How to cite: *Angew. Chem. Int. Ed.* **2016**, *55*, 6694 – 6697
Angew. Chem. **2016**, *128*, 6806 – 6809

[1] a) R. Jin, *Nanoscale* **2015**, *7*, 1549 – 1565; b) H. Qian, M. Zhu, Z. Wu, R. Jin, *Acc. Chem. Res.* **2012**, *45*, 1470 – 1479; c) P. Maity, S. Xie, M. Yamauchi, T. Tsukuda, *Nanoscale* **2012**, *4*, 4027 – 4037.

[2] B. S. Gutrath, I. M. Oppel, O. Presly, I. Beljakov, V. Meded, W. Wenzel, U. Simon, *Angew. Chem. Int. Ed.* **2013**, *52*, 3529 – 3532; *Angew. Chem.* **2013**, *125*, 3614 – 3617.

[3] a) X. K. Wan, S. F. Yuan, Z. W. Lin, Q. M. Wang, *Angew. Chem. Int. Ed.* **2014**, *53*, 2923 – 2926; *Angew. Chem.* **2014**, *126*, 2967 – 2970; b) X. K. Wan, W. W. Xu, S. F. Yuan, Y. Gao, X. C. Zeng, Q. M. Wang, *Angew. Chem. Int. Ed.* **2015**, *54*, 9683 – 9686; *Angew. Chem.* **2015**, *127*, 9819 – 9822.

[4] a) S. Knoppe, T. Bürgi, *Acc. Chem. Res.* **2014**, *47*, 1318 – 1326; b) N. Barrabés, B. Zhang, T. Bürgi, *J. Am. Chem. Soc.* **2014**, *136*, 14361 – 14364.

[5] a) Y. Chen, C. Zeng, D. R. Kauffman, R. Jin, *Nano Lett.* **2015**, *15*, 3603 – 3609; b) M. B. Li, S. K. Tian, Z. Wu, *Nanoscale* **2014**, *6*, 5714 – 5717; c) C. Yao, Y. J. Lin, J. Yuan, L. Liao, M. Zhu, L. H. Weng, J. Yang, Z. Wu, *J. Am. Chem. Soc.* **2015**, *137*, 15350 – 15353.

[6] a) Y. Wang, H. Su, C. Xu, G. Li, L. Gell, S. Lin, Z. Tang, H. Häkkinen, N. Zheng, *J. Am. Chem. Soc.* **2015**, *137*, 4324 – 4327; b) J. Yan, H. Su, H. Yang, S. Malola, S. Lin, H. Häkkinen, N. Zheng, *J. Am. Chem. Soc.* **2015**, *137*, 11880 – 11883; c) Y. B. Song, F. Y. Fu, J. Zhang, J. S. Chai, X. Kang, P. Li, S. L. Li, H. P. Zhou, M. Zhu, *Angew. Chem. Int. Ed.* **2015**, *54*, 8430 – 8434; *Angew. Chem.* **2015**, *127*, 8550 – 8554; d) J. Xiang, P. Li, Y. B. Song, X. Liu, H. B. Chong, S. Jin, Y. Pei, X. Y. Yuan, M. Zhu, *Nanoscale* **2015**, *7*, 18278 – 18283; e) M. S. Bootharaju, C. P. Joshi, M. R. Parida, O. F. Mohammed, O. M. Bakr, *Angew. Chem. Int. Ed.* **2016**, *55*, 922 – 926; *Angew. Chem.* **2016**, *128*, 934 – 938.

[7] a) A. Das, C. Liu, H. Y. Byun, K. Nobusada, S. Zhao, N. Rosi, R. Jin, *Angew. Chem. Int. Ed.* **2015**, *54*, 3140 – 3144; *Angew. Chem.* **2015**, *127*, 3183 – 3187; b) S. Chen, S. X. Wang, J. Zhong, Y. B. Song, J. Zhang, H. T. Sheng, Y. Pei, M. Zhu, *Angew. Chem. Int. Ed.* **2015**, *54*, 3145 – 3149; *Angew. Chem.* **2015**, *127*, 3188 – 3192.

[8] a) Z. Luo, V. Nachammai, B. Zhang, N. Yan, D. T. Leong, D.-e. Jiang, J. Xie, *J. Am. Chem. Soc.* **2014**, *136*, 10577 – 10580; b) N. Goswami, K. Zheng, J. Xie, *Nanoscale* **2014**, *6*, 13328 – 13347.

[9] a) Y. Niihori, M. Matsuzaki, C. Uchida, Y. Negishi, *Nanoscale* **2014**, *6*, 7889 – 7896; b) Y. Niihori, M. Matsuzaki, T. Pradeep, Y. Negishi, *J. Am. Chem. Soc.* **2013**, *135*, 4946 – 4949; c) A. Ghosh, J. Hassinen, P. Pulkkinen, H. Tenhu, R. H. A. Ras, T. Pradeep, *Anal. Chem.* **2014**, *86*, 12185 – 12190; d) J. Hassinen, P. Pulkkinen, E. Kalenius, T. Pradeep, H. Tenhu, H. Häkkinen, R. H. A. Ras, *J. Phys. Chem. Lett.* **2014**, *5*, 585 – 589.

[10] G. Li, R. Jin, *Acc. Chem. Res.* **2013**, *46*, 1749 – 1758.

[11] J. D. Erickson, E. G. Mednikov, S. A. Ivanov, L. F. Dahl, *J. Am. Chem. Soc.* **2016**, *138*, 1502 – 1505.

[12] Y. Chen, C. Liu, Q. Tang, C. Zeng, T. Higaki, A. Das, D.-e. Jiang, N. L. Rosi, R. Jin, *J. Am. Chem. Soc.* **2016**, *138*, 1482 – 1485.

[13] Y. Chen, C. Zeng, C. Liu, K. Kirschbaum, C. Gayathri, R. R. Gil, N. L. Rosi, R. Jin, *J. Am. Chem. Soc.* **2015**, *137*, 10076 – 10079.

[14] a) C. Zeng, Y. Chen, K. Kirschbaum, K. Appavoo, M. Y. Sfeir, R. Jin, *Sci. Adv.* **2015**, *1*, e1500045; b) C. Zeng, Y. Chen, C. Liu, K. Nobusada, N. L. Rosi, R. Jin, *Sci. Adv.* **2015**, *1*, e1500425.

[15] S. Wang, S. Jin, S. Yang, S. Chen, Y. Song, J. Zhang, M. Zhu, *Sci. Adv.* **2015**, *1*, e1500441.

[16] J.-i. Nishigaki, R. Tsunoyama, H. Tsunoyama, N. Ichikuni, S. Yamazoe, Y. Negishi, M. Ito, T. Matsuo, K. Tamao, T. Tsukuda, *J. Am. Chem. Soc.* **2012**, *134*, 14295 – 14297.

[17] a) P. J. Krommenhoek, J. Wang, H. Nathaniel, A. C. Johnston-Peck, K. A. Kozek, G. Kalyuzhny, J. B. Tracy, *ACS Nano* **2012**, *6*, 4903 – 4911; b) D. Crasto, A. Dass, *J. Phys. Chem. C* **2013**, *117*, 22094 – 22097.

[18] D. M. P. Mingos, *Dalton Trans.* **2015**, *44*, 6680 – 6695.

[19] A. Das, C. Liu, C. Zeng, G. Li, T. Li, N. L. Rosi, R. Jin, *J. Phys. Chem. A* **2014**, *118*, 8264 – 8269.

[20] C. Zeng, Y. Chen, A. Das, R. Jin, *J. Phys. Chem. Lett.* **2015**, *6*, 2976 – 2986.

[21] D. Crasto, S. Malola, G. Brosofsky, A. Dass, H. Häkkinen, *J. Am. Chem. Soc.* **2014**, *136*, 5000 – 5005.

[22] H. Yang, Y. Wang, A. J. Edwards, J. Yan, N. Zheng, *Chem. Commun.* **2014**, *50*, 14325 – 14327.

[23] H. Qian, R. Jin, *Chem. Mater.* **2011**, *23*, 2209 – 2217.

[24] A. Das, T. Li, K. Nobusada, C. Zeng, N. L. Rosi, R. Jin, *J. Am. Chem. Soc.* **2013**, *135*, 18264 – 18267.

[25] C. Zhang, R. J. Macfarlane, K. L. Young, C. H. J. Choi, L. Hao, E. Auyeung, G. Liu, X. Zhou, C. A. Mirkin, *Nat. Mater.* **2013**, *12*, 741 – 746.

[26] a) D. M. Chevrier, A. Chatt, P. Zhang, C. Zeng, R. Jin, *J. Phys. Chem. Lett.* **2013**, *4*, 3186 – 3191; b) P. Zhang, *J. Phys. Chem. C* **2014**, *118*, 25291 – 25299.

[27] L. Cheng, Y. Yuan, X. Zhang, J. Yang, *Angew. Chem. Int. Ed.* **2013**, *52*, 9035 – 9039; *Angew. Chem.* **2013**, *125*, 9205 – 9209.

[28] S. Knoppe, S. Malola, L. Lehtovaara, T. Bürgi, H. Häkkinen, *J. Phys. Chem. A* **2013**, *117*, 10526 – 10533; b) S. A. Ivanov, I. Arachchige, C. M. Aikens, *J. Phys. Chem. A* **2011**, *115*, 8017 – 8031.

[29] C. Zeng, H. Qian, T. Li, G. Li, N. L. Rosi, B. Yoon, R. N. Barnett, R. L. Whetten, U. Landman, R. Jin, *Angew. Chem. Int. Ed.* **2012**, *51*, 13114 – 13118; *Angew. Chem.* **2012**, *124*, 13291 – 13295.

[30] X. K. Wan, S. F. Yuan, Q. Tang, D.-e. Jiang, Q. M. Wang, *Angew. Chem. Int. Ed.* **2015**, *54*, 5977 – 5980; *Angew. Chem.* **2015**, *127*, 6075 – 6078.

[31] Z. Tian, L. Cheng, *Nanoscale* **2016**, *8*, 826 – 834.

[32] C. Zeng, T. Li, A. Das, N. L. Rosi, R. Jin, *J. Am. Chem. Soc.* **2013**, *135*, 10011 – 10013.

[33] a) R. Ouyang, D.-e. Jiang, *J. Phys. Chem. C* **2015**, *119*, 21555 – 21560; b) K. L. Dimuthu, M. Weerawardene, C. M. Aikens, *J. Phys. Chem. C*, **2016**, DOI: 10.1021/acs.jpcc.6b01011.

[34] C. Liu, T. Li, G. Li, K. Nobusada, C. Zeng, G. Pang, N. L. Rosi, R. Jin, *Angew. Chem. Int. Ed.* **2015**, *54*, 9826 – 9829; *Angew. Chem.* **2015**, *127*, 9964 – 9967.

[35] D. Crasto, G. Barcaro, M. Stener, L. Sementa, A. Fortunelli, A. Dass, *J. Am. Chem. Soc.* **2014**, *136*, 14933 – 14940.

Received: February 24, 2016
Published online: April 21, 2016

